TELKOMNIKA, Vol. 11, No. 5, May 2013, pp. 2371~ 2376
ISSN: 2302-4046

Linear Analysis for Performance of Dual Mass Flywheel with Centrifugal Pendulum Vibration Absorbers System

Guangming Zhao*, Zhengfeng Jiang, Lei Chen
[1]Department of Electrical Engineering, Wuhan University of Technology, Wuhan
Corresponding author, e-mail: zgmbright@163.com, jzf194901@163.com, chenlei811001@163.com

Abstract

In this study we have offered an investigation of DMF-CPVAs setup for isolating torsional vibration from engine. The simplified mathematical model of DMF-CPVAs setup is built based on the linear theory, the performance of the setup is analyzed, and the result shows that using CPVAs on the DMF leads to an advantage of isolation vibration, instead of just damping vibrations at a specific frequency, could dampen vibrations over a range of frequencies.

Keywords: *torsional vibrations, centrifugal pendulum vibration absorbers, dual mass flywheel*

1. Introduction

In the car engine, torsional vibrations in the crankshaft has been posed as a problem since the torque from the cylinders are delivered in pulses to the crankshaft. This causes the crankshaft to rotate with non-constant speed. These torque pulses are not desirable in the engine because of vibrations that cause even failure of powertrain components. For some years now a special type of flywheel, called the Dual Mass Flywheel (DMF), has been used in powertrains of cars to protect the transmission and the rest of the driveline from engine vibration, see the work of Albers [1]. However DMF remove the resonance frequency below the idle speed, they are tuned to a particular frequency and will not work at all engine speeds.

The Centrifugal Pendulum Vibration Absorbers (CPVAs) is particularly useful for engines since it is not dependent on frequency, but the order of the applied torque. The CPVA can therefore reduce vibrations in the entire engine speed range [2]. But the problem automotive manufacturers face today, is that engines generally tend to become smaller in size and have fewer cylinders, while the power output tend to increase. In order to solve the weakness of DMF and CPVA, the CPVAs are used on the DMF. In this paper, the linear torsional damping characteristic of the DMF-CPVAs setup is investigated.

Figure 1. The structure of DMF-CPVAs setup

Received December 27, 2012; Revised March 4, 2013; Accepted March 14, 2013

2. Derivation of Equation of Motion

A DMF from German manufacturer LuK is shown in Figure 1. The leftmost part is the secondary flywheel, connects to the clutch and transmission The arc spring connects the primary flywheel to the secondary flywheel,. The CPVAs (arc-shaped on the middle carrier) are attached to a separate carrier, which is attached to the secondary flywheel. In this model, the number of CPVAs is eight (four on each side of the carrier). The primary flywheel, rightmost in the picture, attached to the crankshaft.

For deriving the equations of motion, the mathematical model of the DMF-CPVAs setup is simplified, assuming CPVAs work synchronously. The equation of motion equipped with a torsional, frequency tuned vibration absorber, which itself has a circular path CPVA attached to it, will be derived using Lagrange's method. Referring to Figure 2, the kinetic and potential energy will be derived for the system, and will be used to get the equations of motion. Relevant physical parameters labeled in Figure 2 are described in Table 1.

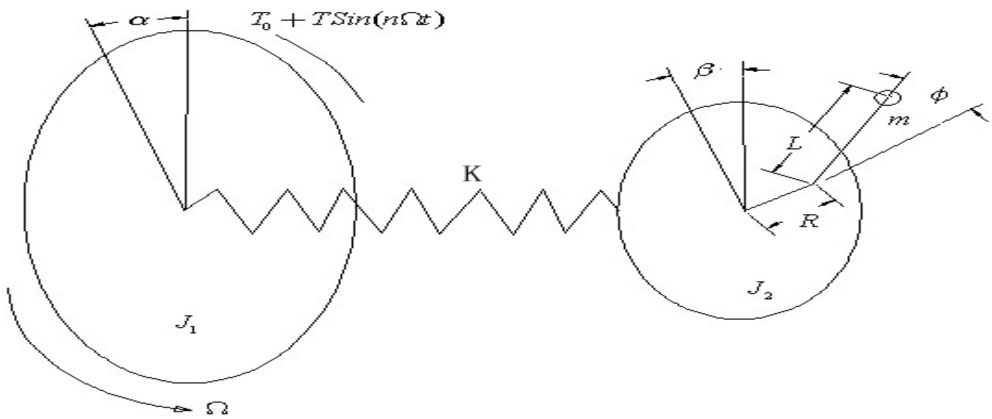

Figure 2. Schematic of DMF-CPVA setup

The total kinetic energy of the system (T_t) consist of that of the 1st flywheel, T_1, the 2nd flywheel T_2, and the CPVA, T_p. $T_t = T_1 + T_2 + T_p$. Defining the individual kinetic energies, we have,

$$T_1 = \frac{1}{2}J_1\dot{\alpha}^2 \quad T_2 = \frac{1}{2}J_2\dot{\beta}^2 \quad T_p = \frac{1}{2}J_p(\dot{\beta} + \dot{\phi})^2 + \frac{1}{2}m_p\dot{\vec{r}}\cdot\dot{\vec{r}}$$

where, $\dot{\vec{r}}$ the time rate of change of the position vector from the center of the torsional absorber to the pendulum center of mass. We will derive the position vector using the coordinate system in Figure 2. We can see that $\vec{r} = R\hat{e}_R + L\hat{e}_L$. Grouping all the terms, letting where ρ is the pendulum's radius of gyration about its center of mass, and performing the dot product gives

$$T_t = \frac{1}{2}J_1\dot{\alpha}^2 \frac{1}{2}J_2\dot{\beta}^2 + \frac{1}{2}m[R^2\dot{\beta}^2 + 2RL\dot{\beta}(\dot{\beta} + \dot{\phi})\cos(\phi) + (L^2 + \rho^2)(\dot{\beta} + \dot{\phi})^2]$$

Next, the potential energy in the system consists of the torsional spring only, and can be found to be

$$V = \frac{1}{2}k(\alpha - \beta)^2$$

Finally, the generalized forces, for the 1st flywheel, 2nd flywheel, and absorbers, which include the damping and the forcing terms, can be found to be

$$Q_\alpha = -c_\alpha \dot{\alpha} + T_0 + T\sin(n\Omega t),$$
$$Q_\beta = c_p \dot{\varphi}\cos(\varphi) - c_\beta \dot{\beta},\quad Q_\varphi = -c_p \dot{\varphi}$$

Terms in the generalized forces are as follow: cp is the viscous damping in the pendulum bearing, c_α is the 1st flywheel damping, c_β is is the damping on the 2nd flywheel. To is the mean torque applied to the rotor, and $T\sin(n\Omega t)$ is the fluctuating torque applied to the rotor. Now, Lagrange's method can be applied to the kinetic energies and generalized forces to obtain the system's equations of motion. Taking

$$\frac{d}{dt}\left(\frac{\partial T_t}{\partial \dot{\alpha}}\right) - \frac{\partial T_t}{\partial \alpha} + \frac{\partial V}{\partial \alpha} = Q_\alpha$$

gives,

$$J_1 \ddot{\alpha} + k(\alpha - \beta) + c_\alpha \dot{\alpha} = T_0 + T\sin(n\Omega t) \tag{1}$$

as the equation of motion for the 1st flywheel. Proceeding in a similar manner for the β and φ coordinates yields, for the 2nd flywheel's equation of motion, and for the pendulum,

$$(J_2 + mR^2 + m(L^2 + r^2) + 2mRL\cos(\varphi))\ddot{\beta} + m(L^2 + r^2 + RL\cos(\varphi))\ddot{\varphi} - mRL\dot{\varphi}(2\dot{\beta} + \dot{\varphi}) + k(\alpha - \beta) + c_\beta \dot{\beta} - c_p \dot{\varphi}\cos(\varphi) = 0 \tag{2}$$

$$m(L^2 + r^2 + RL\cos(\varphi))\ddot{\beta} + m(L^2 + r^2)\ddot{\varphi} + mRL\sin(\varphi) + c_p \dot{\varphi} = 0 \tag{3}$$

We have derived the equations of motion for the system previously described and the next step is to perform some linear analysis.

Table 1. Definition of Symbols in Figure 2

Symbol	Physical Meaning
α	Rotor angle of the 1st flywheel
β	Rotor angle of the 2nd flywheel
Ω	Rotor speed of the DMF
Φ	Torsional angle of the 2nd flywheel
φ	Absorber's swing angle respect to the 2nd flywheel
R	Distance from the 2nd flywheel to the absorber's center of rotation
L	Distance from the absorber's center of rotation to its center of mass
ρ	Pendulum's radius of gyration about its center of mass
k	Spring stiffness
J_1	Rotational inertial of the 1st flywheel
J_2	Rotational inertial of the 2nd flywheel
J_p	Rotational inertia of the pendulum
m	Mass of the pendulum

3. Linear Analysis

In order to perform linear analysis on the system derived in the previous section, some assumptions must be made. First, we assume small pendulum absorber angles so that the sines and cosines can be approximated. $|\phi| \ll 1$. We also assume small oscillations about a mean speed for the DMF [3].

$$\alpha = \Omega t + \eta_1,\quad \beta = \Omega t + \eta_2$$

Using these assumptions in the full non-linear equations and keeping only the linear terms yields,

$$J_1\ddot{\eta}_1 + k(\eta_1 - \eta_2) + c_a(\Omega + \dot{\eta}_1) = T_0 + T\sin(n\Omega t) \quad (4)$$

$$(J_2 + m(R+L)^2 + mr^2)\ddot{\eta}_2 + m(L^2 + r^2 + RL)\ddot{\phi} + k(\eta_1 - \eta_2) + c_b(\Omega + \dot{\eta}_2) - c_p\dot{\phi} = 0 \quad (5)$$

$$m(L^2 + r^2 + RL)\ddot{\eta}_2 + m(L^2 + r^2)\ddot{\phi} + c_p\dot{\phi} = 0 \quad (6)$$

for the linearized equation of the 1st flywheel, the 2nd flywheel's equation of motion, and for the pendulum separately. Now that the system is linearized, setting the damping and mean torque to zero allows us to assume a harmonic response for each of the degrees of freedom and solve for their respective amplitudes,

$$\eta_1 = a_0\sin(n\Omega t), \quad \eta_2 = b_0\sin(n\Omega t), \quad \phi = \phi_0\sin(n\Omega t)$$

and the system natural frequency without CPVAs,

$$\omega_0 = \sqrt{(kJ_1 + kJ_2)/J_1J_2} \quad (7)$$

Plugging the above assumptions into the linearized equations of motion, assuming a point mass for the absorber to eliminate its moment of inertia, and solving for the amplitudes gives:

$$a_0 = \frac{T(-n^2+\tilde{n}^2)m - n^2T(1+m)(-n^2+\tilde{n}^2+\tilde{n}^2(1+2n^2+\tilde{n}^4)n)\sigma^2}{kn^2(1+m)\sigma^2(-\tilde{n}^2(1+m+n+\tilde{n}^4n)+n^4(1+m)(-1+2\tilde{n}^2n)\sigma^2+n^2(1+m-2\tilde{n}^2n+\tilde{n}^2(1+m)(1+n+\tilde{n}^4n)\sigma^2))}$$

$$b_0 = \frac{-T(n^2-\tilde{n}^2)}{kn^2(1+m)\sigma^2(-\tilde{n}^2(1+m+n+\tilde{n}^4n)+n^4(1+m)(-1+2\tilde{n}^2n)\sigma^2}$$

$$® \frac{m}{+n^2(1+\tilde{n}^6n\sigma^2+m(1+\tilde{n}^6n\sigma^2+\tilde{n}^2(1+n)\sigma^2)+\tilde{n}^2(\sigma^2+n(-2+\sigma^2))))}$$

$$\phi_0 = \frac{T(1+\tilde{n}^2)m}{k(1+m)\sigma^2(-\tilde{n}^2(1+m+n+\tilde{n}^4n)+n^4(1+m)(-1+2\tilde{n}^2n)\sigma^2+n^2(1+m-2\tilde{n}^2n+\tilde{n}^2(1+m)(1+n+\tilde{n}^4n)\sigma^2))}$$

where, $\sigma = \Omega/\omega_0, m = J_1/J_2, n = J_3/J_2$

Take a four-stroke engine as study subject, a torque pulse (also called power-stroke) is delivered once every two revolutions of the engine, from every cylinder. In a four-cylinder engine, the cylinders excite the crankshaft twice every revolution, and therefore the torque has a dominant second order harmonic component. Parameter value k=20N/°, T=40N, R=0.1m, L=0.25m, m=0.5kg, J_1 =0.2kgm^2, J_2=0.08 kgm^2, Ω=300r/min. The amplitude of 2nd flywheel can be seen from Figure 3.

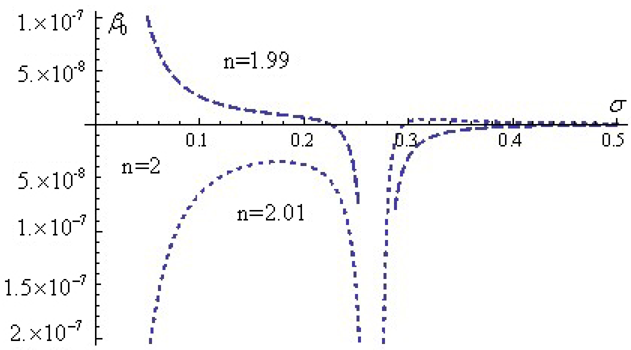

Figure 3. Amplitude of 2nd disk versus σ for different tuning values.

Since the absorber is tuned to one frequency, if the tuning order equal to the excitation order, the amplitude of the 2nd flywheel goes to zero at that frequency, as shown in figure 3. Under the a little detuning, the resonance happens around σ=0.25, which is under idle operating speed of engine. With the speed increasing, the torsional vibration angle reduces to zero.

4. Vibration Isolation Performance

To further investigate the high frequency resonance for the DMF-CPVAs setup system, neglecting damping items, the three natural frequencies of the system were solved for using the standard method. $|K\text{-}\omega^2 M|=0$, and solving for the ω

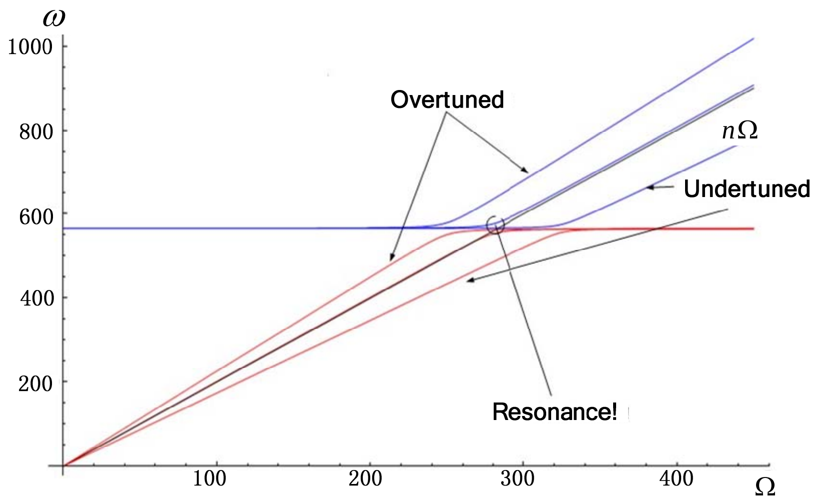

Figure 4. DMF-CPVAs setup system natural frequencies vs. rotor mean speed

For tuning the excitation order, which is shown in a Campbell diagram in Figure 4, we know one frequency is at zero, and the other two are plotted vs. the mean rotor speedΩ, for different CPVA tunings. The forcing frequency, nΩ is also plotted in Figure 4, and it is obvious that an intersection of the forcing line with a natural frequency line indicates a resonance. There are three sets of the two natural frequencies plotted in this Figure 4, one indicates a highly undertuned CPVA, one a highly overtuned CPVA, and one an exactly tuned CPVA. The case for the exactly tuned CPVA is not labeled and is the lines which almost exactly follow the forcing function.

Campbell diagram in Figure 4 exhibit a classical eigenvalue veering behavior [4]. The resonance happens around 300 r/min, no resonance happens in engine operating speed. We can see DMF-CPVAs system performs good isolation effect, and removes the resonance which happens in higher frequency.

Plotted in Figure 5 is the amplitude of the rotor for three different absorber setups using the linear theory as a function of frequency, torsional absorber only, DMF system, and CPVA only, these systems all have the same total rotary inertia. As is visible from the Figure, the torsional absorber is the least effective setup, having an anti-resonance at one frequency only, the DMF setup absorbers torsional vibrations more effectively at lower frequencies than the CPVA only setup, but does have a resonance at higher frequency which could be detrimental to performance. The CPVA only system has a resonance at ω=0 just like the other two, but has the benefit of no more resonances at high frequencies, but the CPVA only system can't be built as same rotary inertia as DMF on crankshaft in practice.

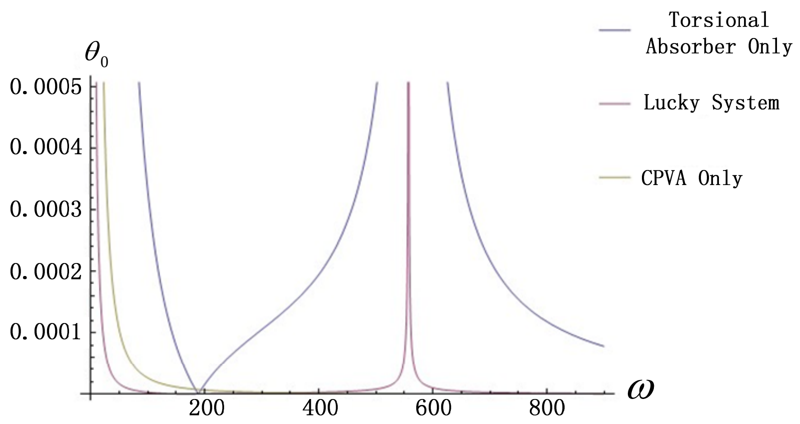

Figure 5. Rotor amplitude vs. frequency for three absorber setups.

5. Conclusions and Future work

In the work, the equations of motion for DMF-CPVAs setup model were established. It should be pointed out though, that the model was much simplified, especially on the secondary side. The clutch, gearbox, differential, driveshaft and other parts are not built and significant effects might be missed. According to linear analysis, the torsional vibration isolation performance was investigated under different tuning modes, and the result shows the implementation of CPVAs on the DMF that will account for additional total torsional vibration reduction effect. Further work could also include the nonlinear analysis for DMF-CPVAs setup to study existence and stability of response and performing experimental tests in a car.

Acknowledgements

This work was done at Michigan State University. The authors are grateful to Steven W. Shaw and Brendan J. Vidmar for many discussions that contributed to this work.

References

[1] A Albers. Advanced Development of Dual Mass Flywheel (DMFW) Design - Noise Control for Today's Automobiles.
[2] W Ker Wilson. Practical Solution of Torsional Vibration Problem, Chapter XXX. Vol. IV. Champman and Hall Ltd, London. 1968.
[3] Alsuwaiyan AS. "Performance, stability, and localization of systems of vibration absorbers". PhD Thesis, Michigan State University. 1999.
[4] Pierre C. "Mode Localization and Eigen value Loci Veering Phenomena in Disordered Structures". *J. Sound Vib*. 1988; 126(3): 485–502.